Supporting Information

A Metal-Organic Framework Adsorbent for Practical Capture of Trace Carbon Dioxide

Jinkyoung Park,[†,⊥] Jeoung Ryul Park,[†,⊥] Jong Hyeak Choe,[†] Saemi Kim,[‡] Minjung Kang,[†] Dong Won Kang,[†] Jee Yeon Kim,[‡] Yong Won Jeong,[‡] and Chang Seop Hong[*,†]

†Department of Chemistry, Korea University, Seoul 02841, Republic of Korea
‡Samsung Research, SEC, 33, Seongchon-gil, Seocho-gu, Seoul, Korea
[⊥]J.P. and J.R.P. contributed equally.

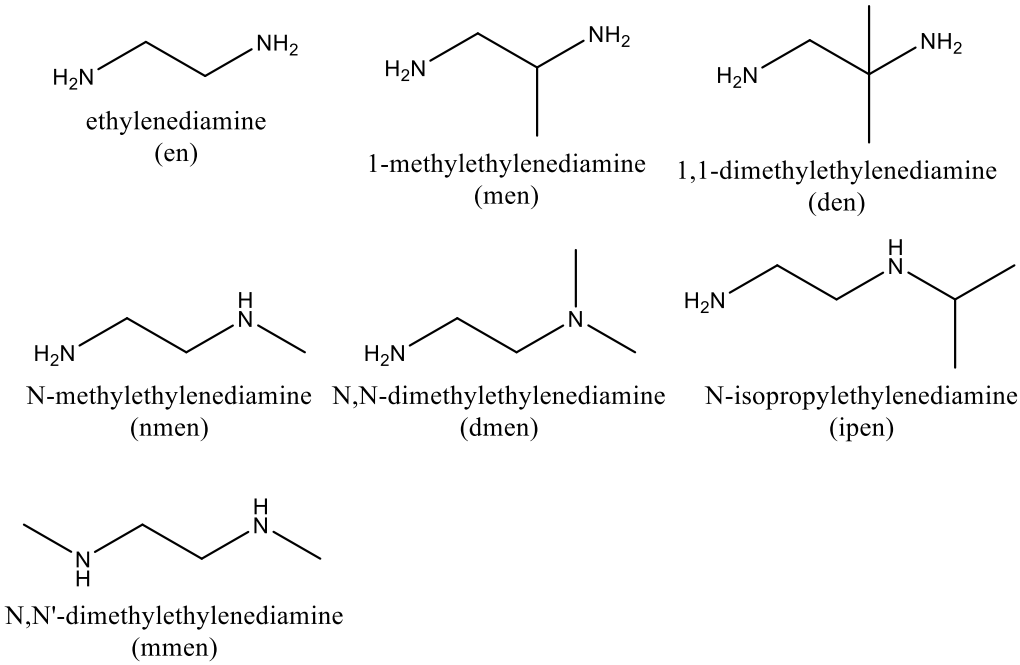

(a)

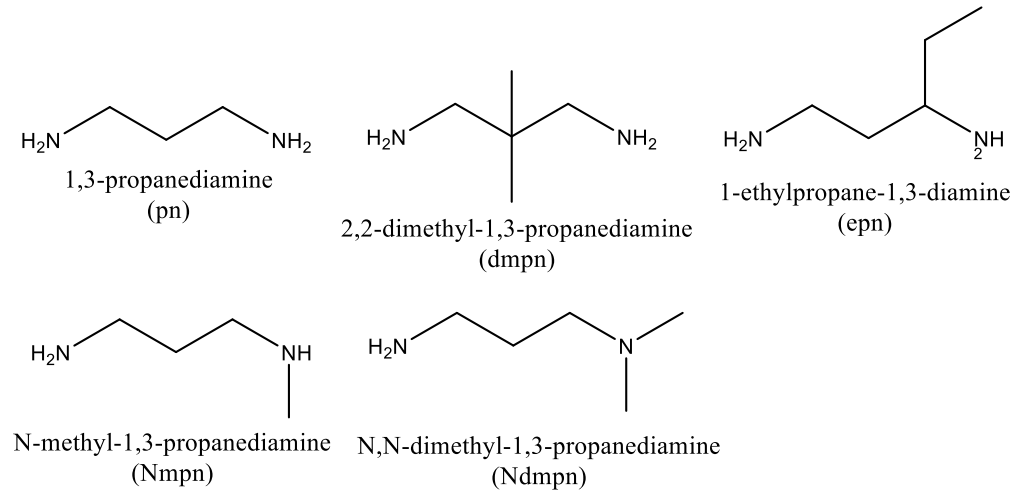

(b)

Figure S1. (a) Diamines with an ethylene linker. (b) Diamines with a propylene linker.

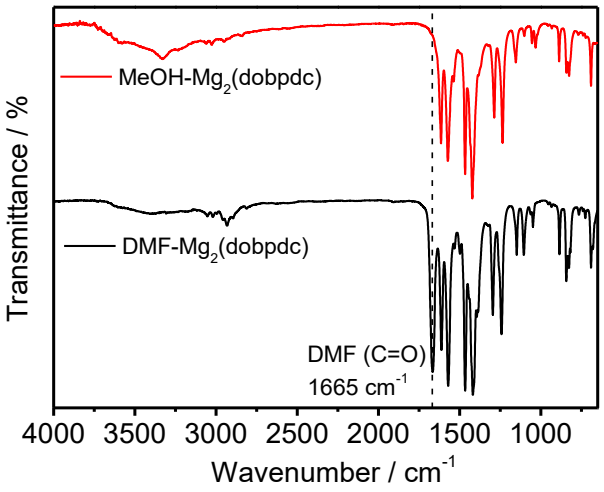

Figure S2. IR spectra of as-prepared and MeOH-exchanged Mg_2(dobpdc). The characteristic peak at 1665 cm^{-1}, assigned to C=O vibration of DMF, disappeared when as-prepared Mg_2(dobpdc) was soaked in MeOH. This indicates that DMF molecules in the pores and coordinated to Mg^{2+} ions were replaced by MeOH.

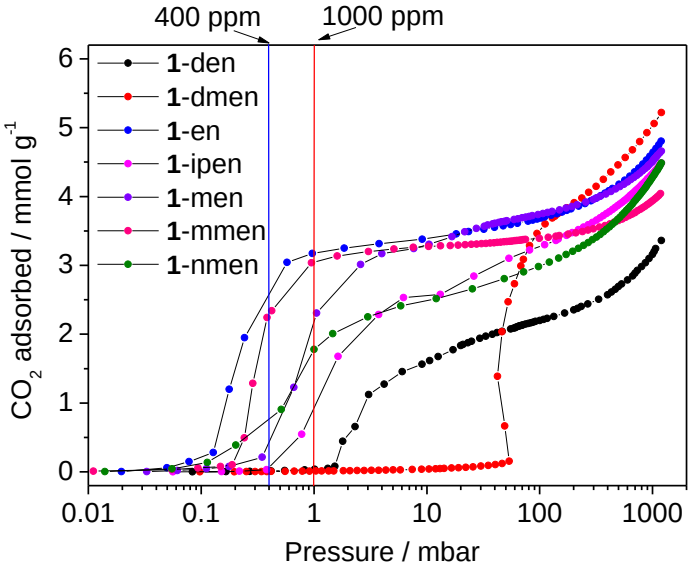

Figure S3. CO_2 isotherms of diamine-functionalized **1** with ethylene links at 25 °C.[1-5]

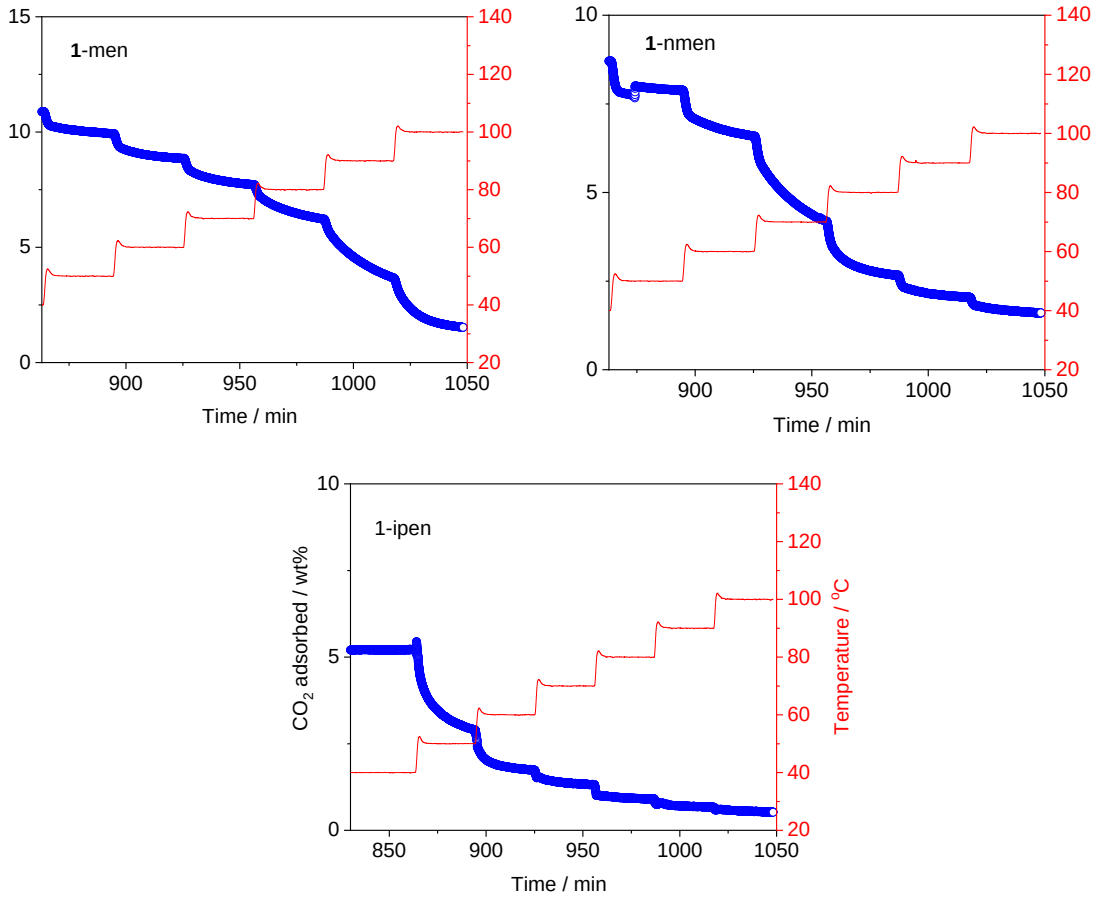

Figure S4. Adsorption of selected EDA-grafted **1** at 1000 ppm CO_2 with increasing temperature.

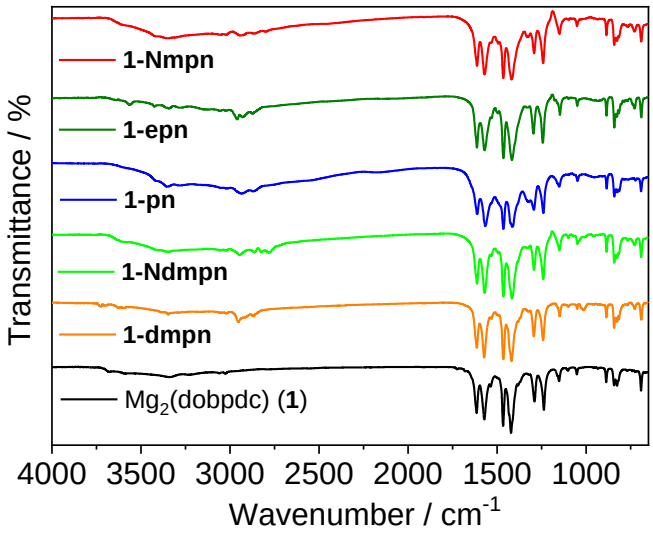

Figure S5. IR spectra of diamine-functionalized Mg_2(dobpdc) samples.

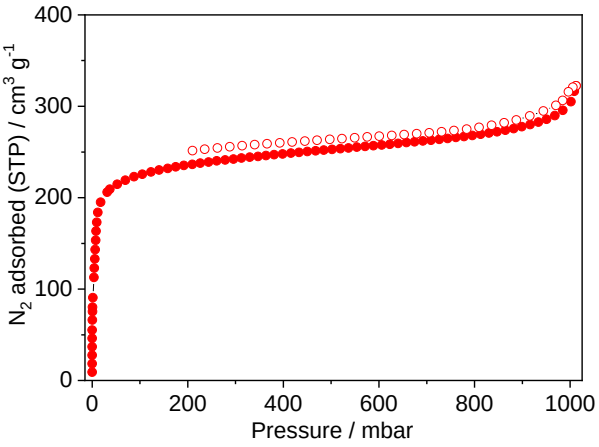

(a)

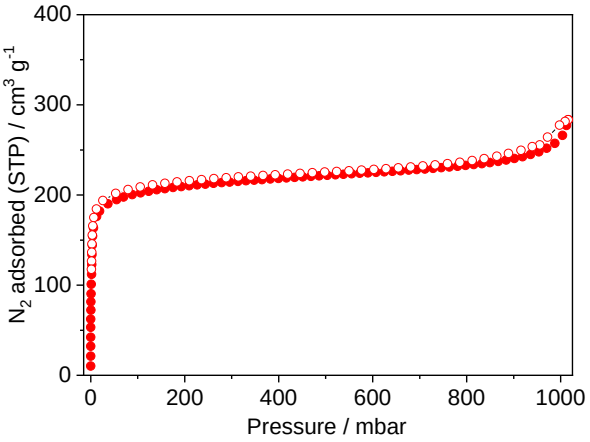

(b)

Figure S6. N_2 isotherms of (a) **1-Nmpn** and (b) **1-epn** at 77 K.

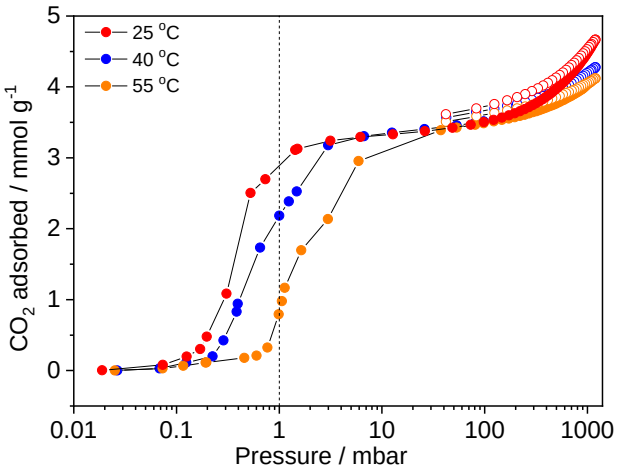

(a)

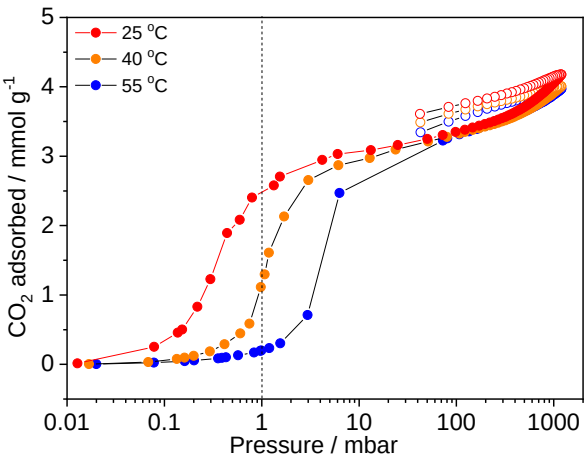

(b)

Figure S7. CO_2 isotherms of (a) **1-Nmpn** and (b) **1-epn** at the indicated temperatures.

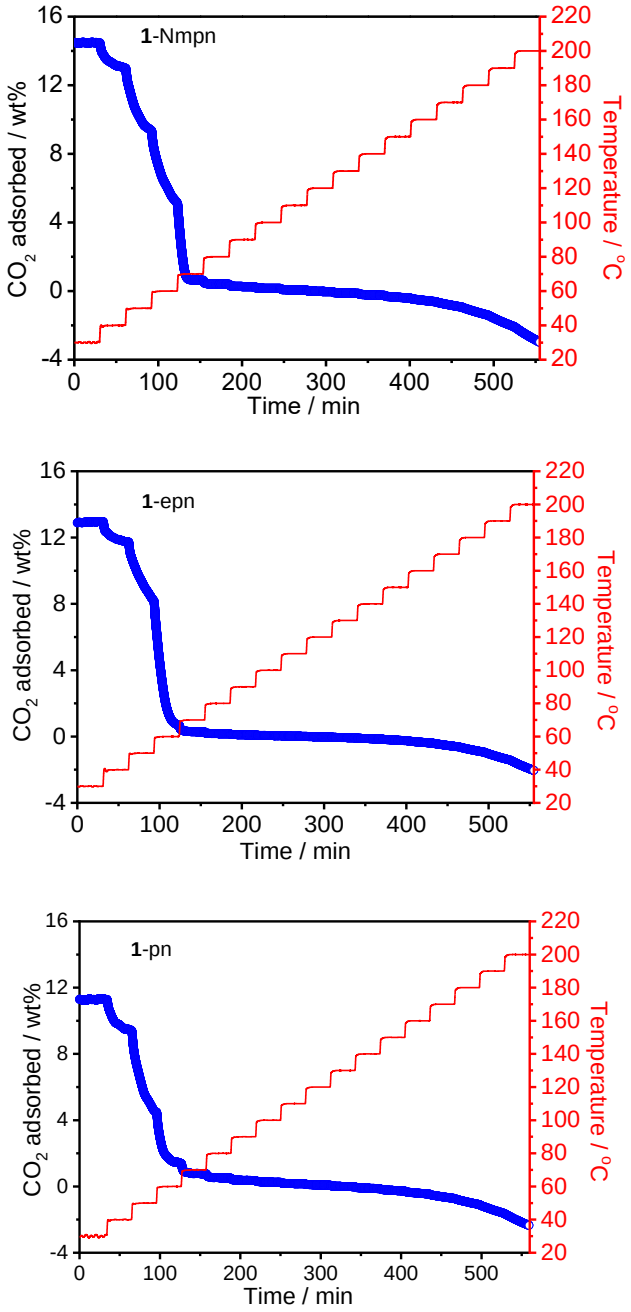

Figure S8. Adsorption of **1-Nmpn**, **1-epn** and **1-pn** at 1000 ppm CO_2 with increasing temperature.

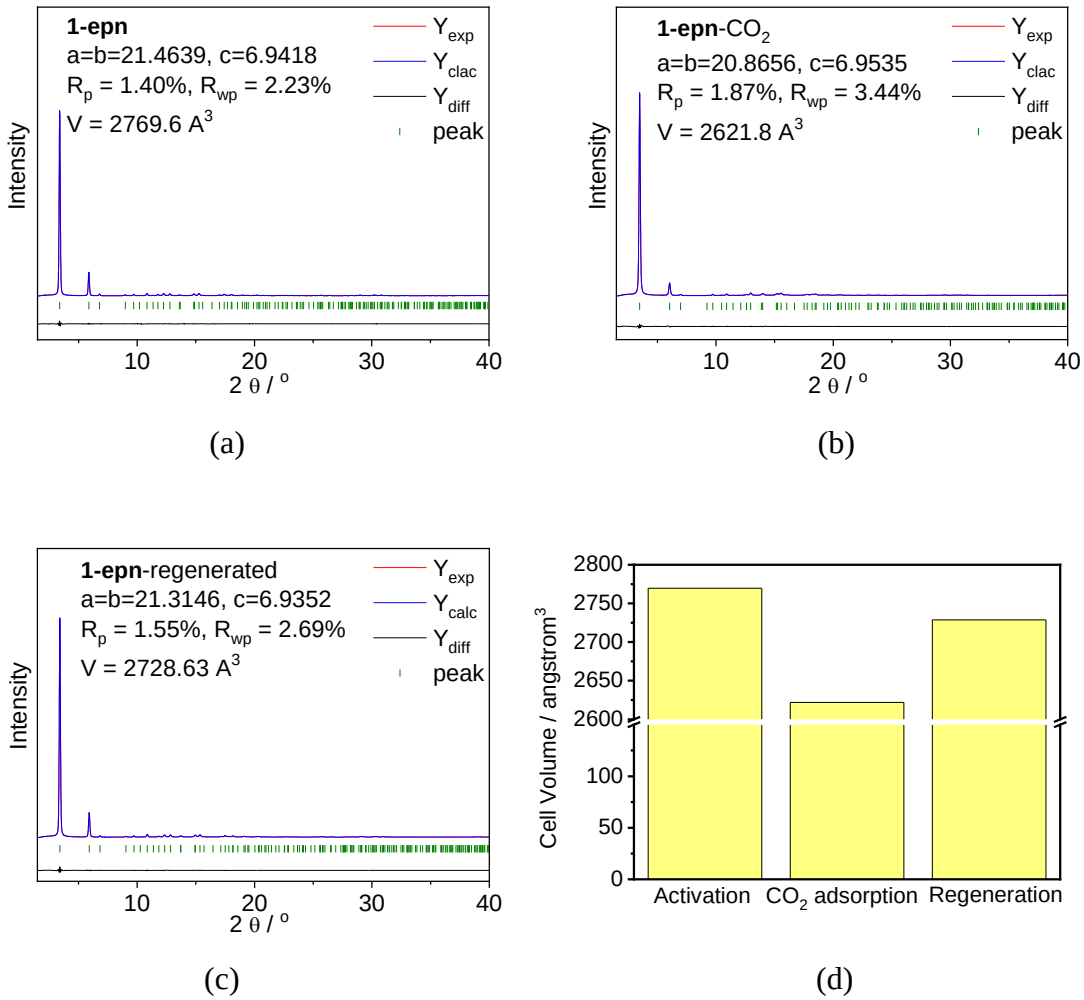

Figure S9. Synchrotron powder X-ray diffraction pattern of **1-epn** (a) after activation, (b) after CO_2 adsorption, (c) after regeneration at 70 ºC. (d) Comparison of cell volume of **1-epn** under different conditions.

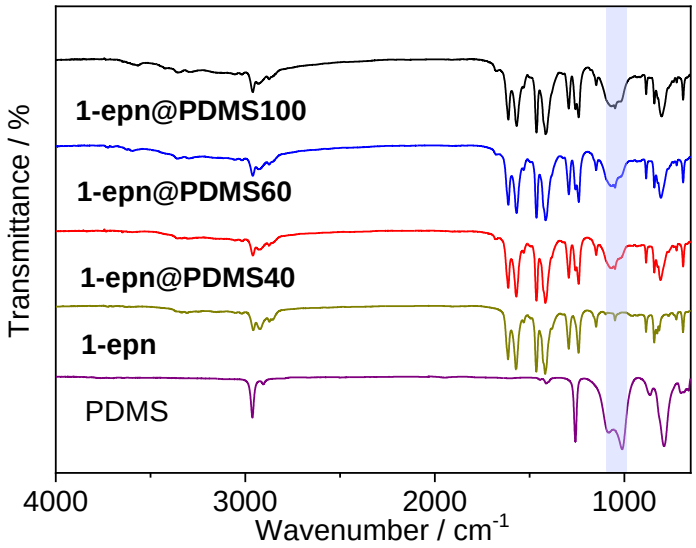

Figure S10. IR spectra of PDMS, **1-epn**, and PDMS-coated samples.

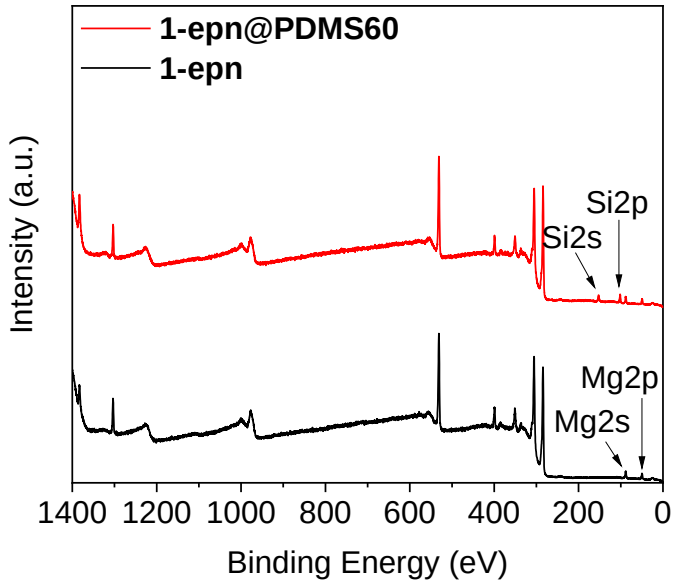

Figure S11. XPS data of **1-epn** and **1-epn@PDMS60**.

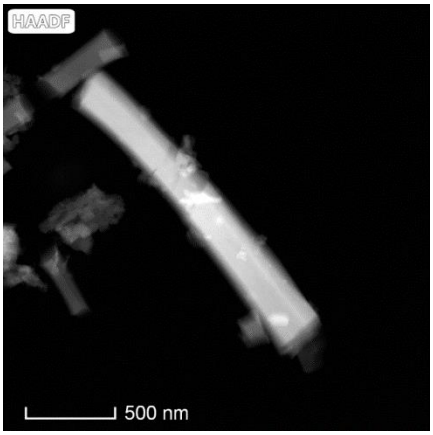

(a)

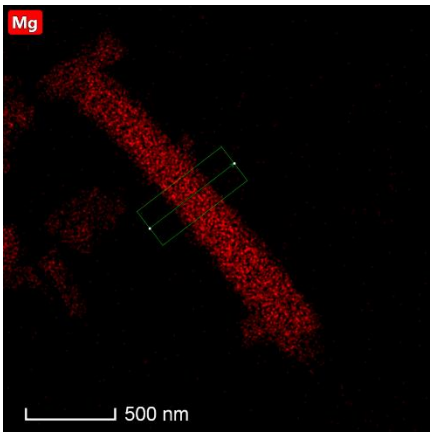

(b)

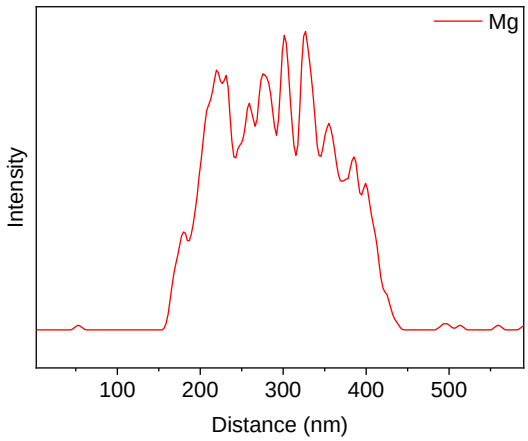

(c)

Figure S12. (a) STEM image, (b) elemental mapping analysis, and (c) cross-sectional area-scan profile of **1-epn**.

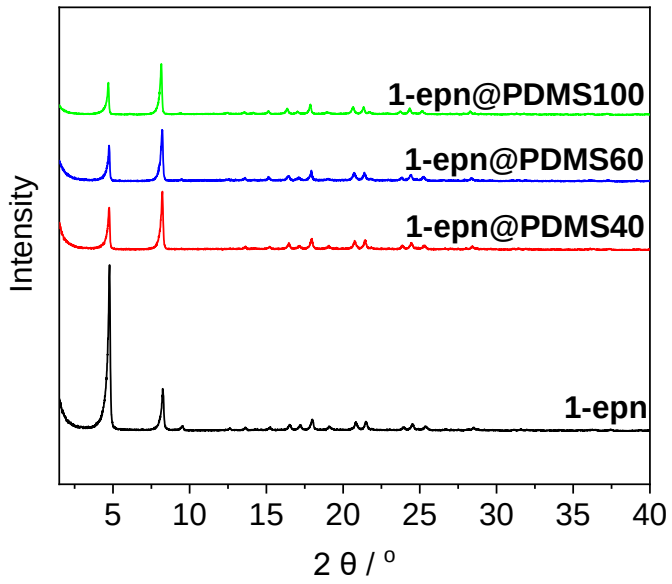

Figure S13. PXRD patterns of **1-epn** and PDMS-coated samples.

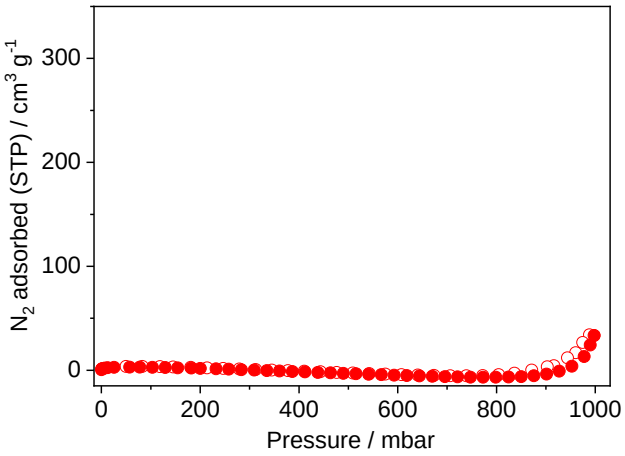

Figure S14. N_2 isotherm of **1-epn@PDMS60** at 77 K.

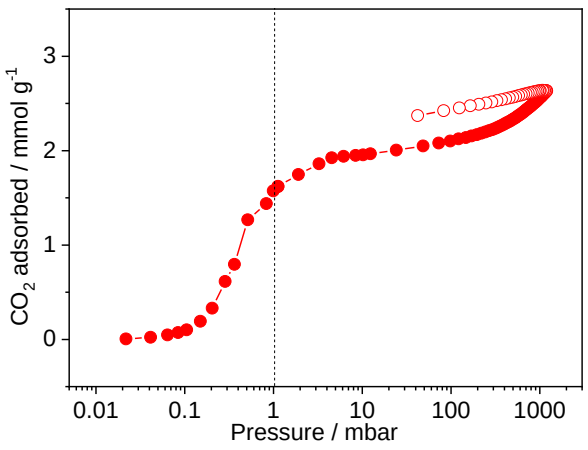

Figure S15. CO_2 isotherm of **1-epn@PDMS60** at 298 K.

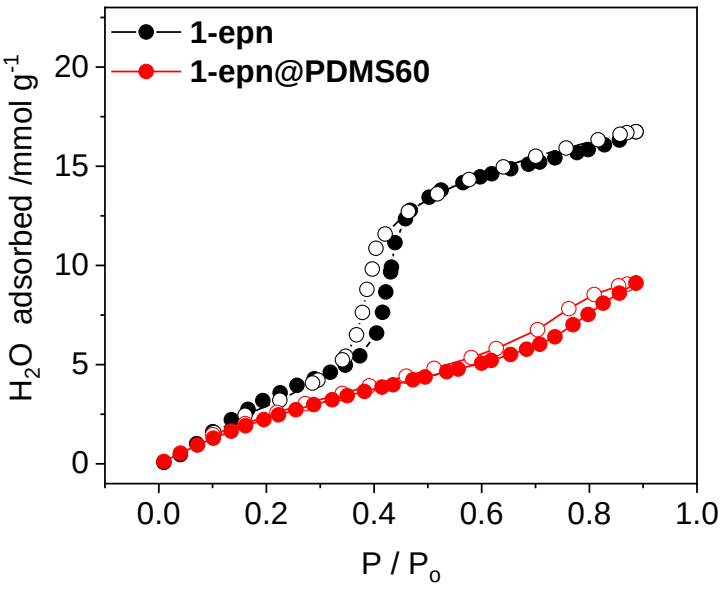

Figure S16. Water adsorption isotherms of **1-epn** and **1-epn@PDMS60** at 25 ºC.

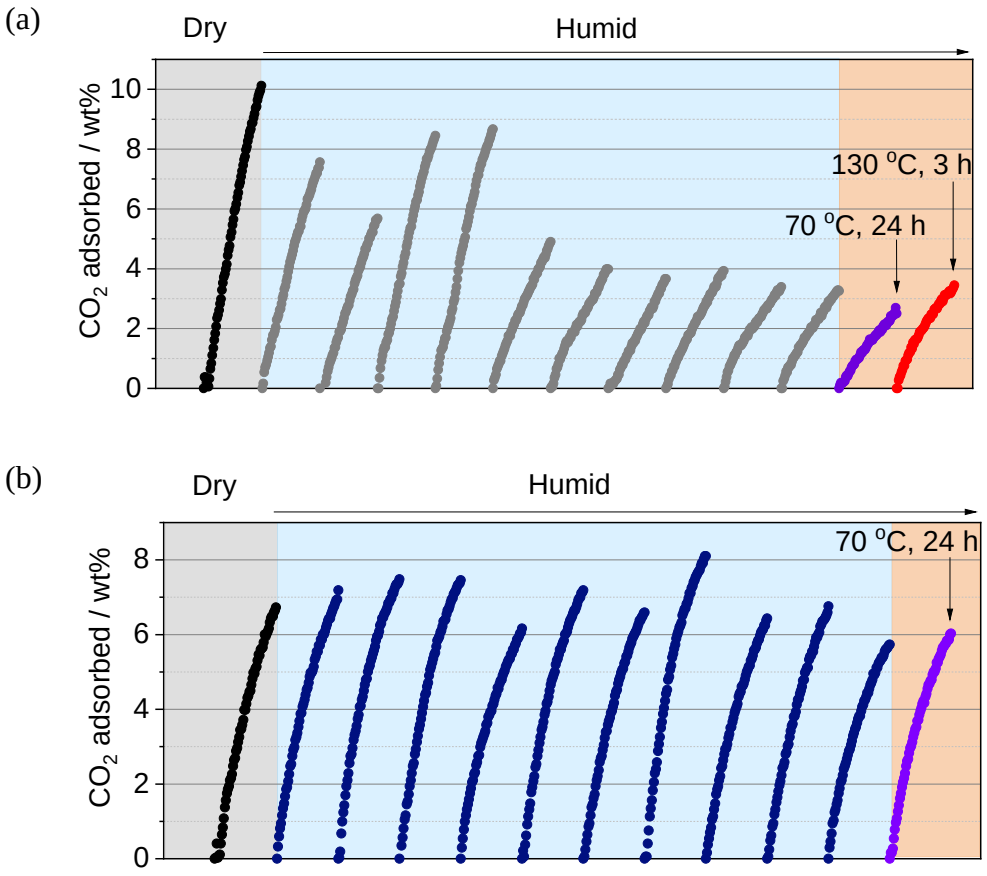

Figure 17. Variation of CO_2 removal capacity in weight percentage by (a) **1-epn** and (b) **1-epn@PDMS60** under dry (25% RH) and humid conditions (60% RH) for 1 h. Regeneration was conducted at 70 °C for 1 h.

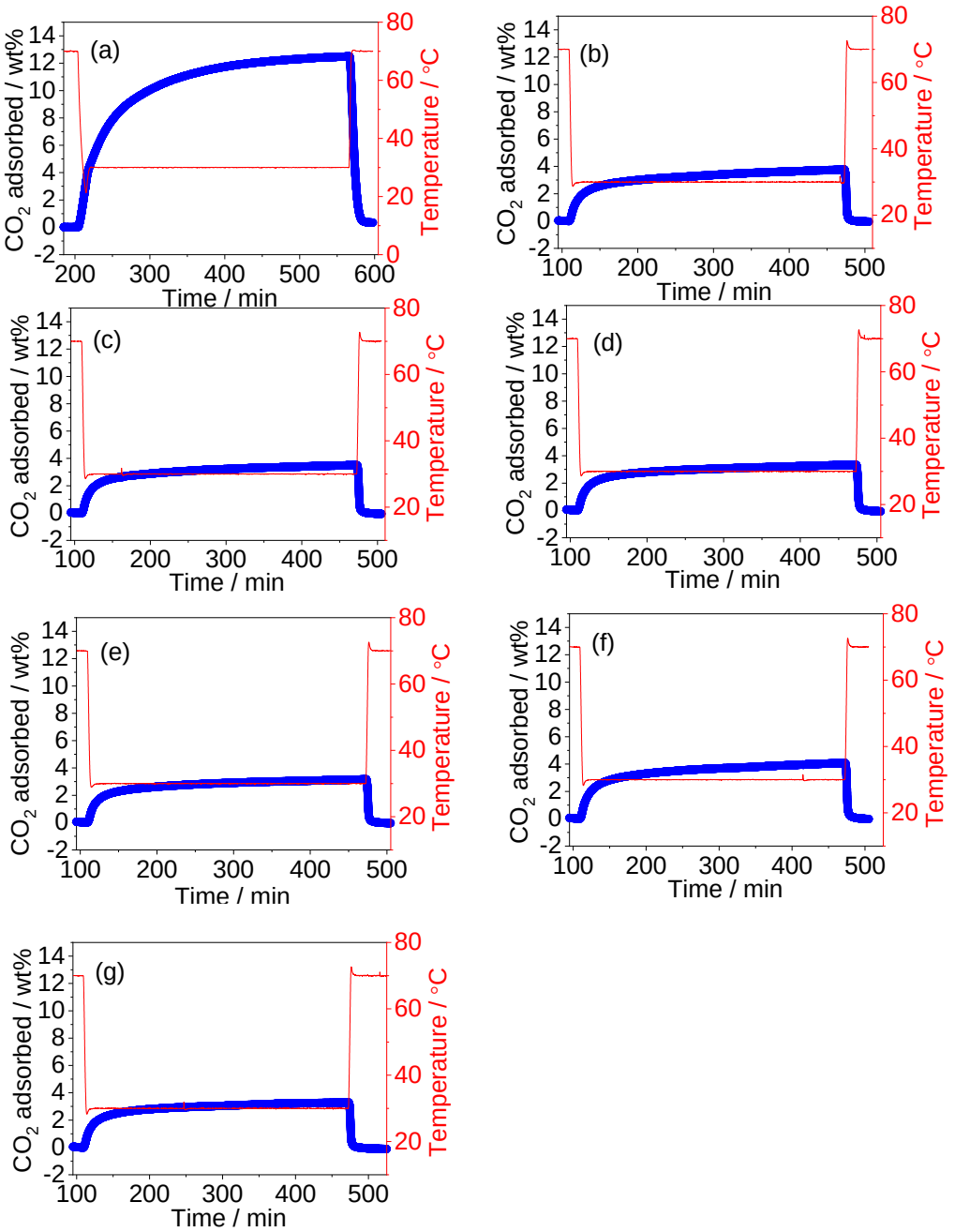

Figure 18. (a) Variation of CO_2 adsorption capacity in weight percentage by **1-epn**. The sample was pre-treated in a stream of N_2 at 140 °C for 2 h. Adsorption occurred in a stream of 1000 ppm CO_2 for 12 h. (b-g) Variation of CO_2 adsorption capacity in weight percentage by **1-epn** from (b) 1st cycle to (g) 6th cycle. The sample was exposed to 98% RH for 12 h and then was regenerated in a stream of 1000 ppm CO_2 at 70 °C for 30 min. For the 1st cycle, adsorption occurred in a stream of 1000 ppm CO_2 for 6 h. The next cycles followed the same procedure.

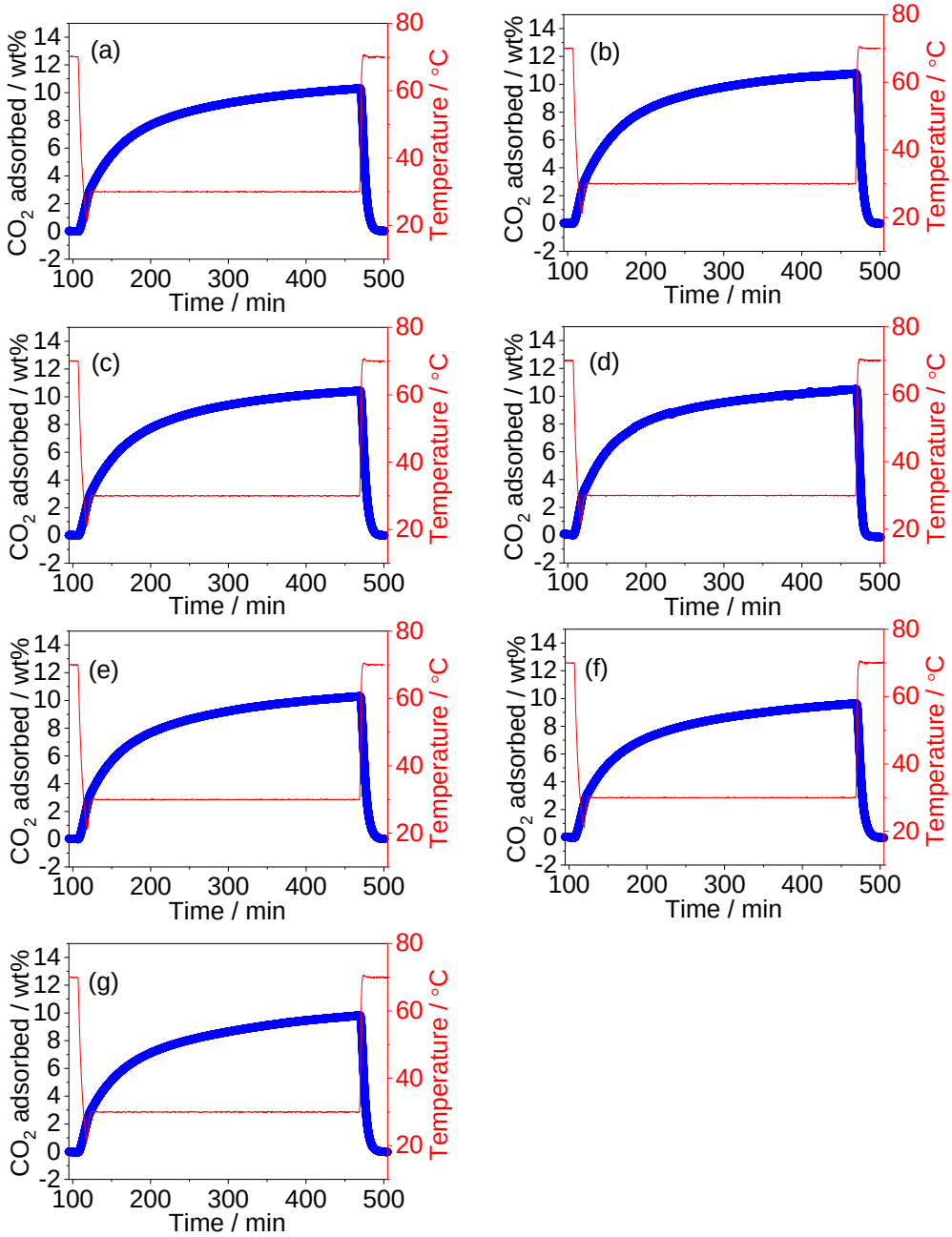

Figure 19. (a) Variation of CO_2 adsorption capacity in weight percentage by **1-epn@PDMS60**. The sample was pre-treated in a stream of N_2 at 140 °C for 2 h. Adsorption occurred in a stream of 1000 ppm CO_2 for 12 h. (b-g) Variation of CO_2 adsorption capacity in weight percentage by **1-epn@PDMS60** from (b) 1st cycle to (g) 6th cycle. The sample was exposed to 98% RH for 12 h and then was regenerated in a stream of 1000 ppm CO_2 at 70 °C for 30 min. For the 1st cycle, adsorption occurred in a stream of 1000 ppm CO_2 for 6 h. The next cycles followed the same procedure.

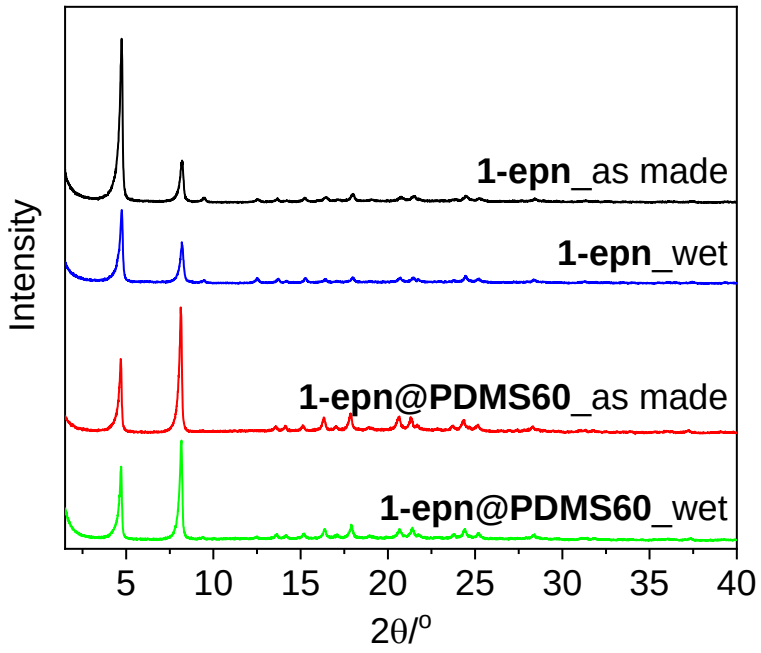

Figure S20. PXRD patterns of **1-epn** and **1-epn@PDMS60** before and after 6 cyclic exposures to 95% RH.

Table S1. Adsorption capacities at 400 and 1000 ppm CO_2, and the difference between two values. Data was obtained from adsorption isotherms at 25 °C.

Materials	Uptake amount at 400 ppm (wt%)	Uptake amount at 1000 ppm (wt%)	Difference	Ref.
BaMFI	3.5	3.93	0.43	[6]
SrMFI	3.38	3.77	0.39	[6]
CaMFI	2.38	2.59	0.21	[6]
NaMFI	1.69	2.81	1.12	[6]
TRIPE-MCM-41	4.58	5.3	0.72	[7]
Mg-MOF-74	0.58	1.47	0.89	[8]
Zeolite 13X	1.93	3.34	1.41	[8]
SIFSIX-18-Ni-β	1.57	3.54	1.97	[8]
UIO-66-NH2	0.69	1.77	1.08	[8]
TIFSIX-3-Ni	4.91	7.17	2.26	[8]
NbOFFIVE-1-Ni	5.5	7.53	2.03	[9]
1-epn	7.75	10.95	3.2	This work
1-pn	7.75	12.23	4.48	This work
1-Nmpn	7.75	12.67	4.92	This work
1-en	11.26	13.99	2.73	This work
1-ipen	0.28	4.13	3.85	This work
1-men	1.82	9.66	7.84	This work
1-nmen	3.38	7.83	4.45	This work
1-mmen	10.02	13.44	3.42	This work

Table S2. Adsorption capacities at 40 ºC and 70 ºC, and difference between the two values. Data was obtained uising TGA under 1000 ppm CO_2.

Materials	Uptake amount at 40 ºC (wt%)	Uptake amount at 70 ºC (wt%)	Difference
1-ipen	5.22	1.32	74.77
1-nmen	8.71	4.19	51.89
1-den	6.41	3.20	50.08
1-men	10.88	7.70	29.23
1-Nmpn	12.96	0.63	95.17
1-pn	9.43	0.75	92.03
1-epn	11.74	0.27	97.68

References

(1) Jo, H.; Lee, W. R.; Kim, N. W.; Jung, H.; Lim, K. S.; Kim, J. E.; Kang, D. W.; Lee, H.; Hiremath, V.; Seo, J. G.; Jin, H.; Moon, D.; Han, S. S.; Hong, C. S. Fine-Tuning of the Carbon Dioxide Capture Capability of Diamine-Grafted Metal-Organic Framework Adsorbents Through Amine Functionalization. *ChemSusChem* **2017,** *10* (3), 541-550, DOI: 10.1002/cssc.201601203.
(2) Kang, M.; Kim, J. E.; Kang, D. W.; Lee, H. Y.; Moon, D.; Hong, C. S. A Diamine-Grafted Metal–Organic Framework with Outstanding CO_2 Capture Properties and a Facile Coating Approach for Imparting Exceptional Moisture Stability. *J. Mater. Chem. A* **2019,** *7* (14), 8177-8183, DOI: 10.1039/c8ta07965j.
(3) Lee, W. R.; Hwang, S. Y.; Ryu, D. W.; Lim, K. S.; Han, S. S.; Moon, D.; Choi, J.; Hong, C. S. Diamine-Functionalized Metal–Organic Framework: Exceptionally High CO_2 Capacities from Ambient Air and Flue Gas, Ultrafast CO_2 Uptake Rate, and Adsorption Mechanism. *Energy Environ. Sci.* **2014,** *7* (2), 744-751, DOI: 10.1039/c3ee42328j.
(4) Lee, W. R.; Jo, H.; Yang, L. M.; Lee, H.; Ryu, D. W.; Lim, K. S.; Song, J. H.; Min, D. Y.; Han, S. S.; Seo, J. G.; Park, Y. K.; Moon, D.; Hong, C. S. Exceptional CO_2 Working Capacity in a Heterodiamine-Grafted Metal-Organic Framework. *Chem. Sci.* **2015,** *6* (7), 3697-3705, DOI: 10.1039/c5sc01191d.
(5) Lee, W. R.; Kim, J. E.; Lee, S. J.; Kang, M.; Kang, D. W.; Lee, H. Y.; Hiremath, V.; Seo, J. G.; Jin, H.; Moon, D.; Cho, M.; Jung, Y.; Hong, C. S. Diamine-Functionalization of a Metal-Organic Framework Adsorbent for Superb Carbon Dioxide Adsorption and Desorption Properties. *ChemSusChem* **2018,** *11* (10), 1694-1707, DOI: 10.1002/cssc.201800363.
(6) Itadani, A.; Oda, A.; Torigoe, H.; Ohkubo, T.; Sato, M.; Kobayashi, H.; Kuroda, Y. Material Exhibiting Efficient CO_2 Adsorption at Room Temperature for Concentrations Lower Than 1000 ppm: Elucidation of the State of Barium Ion Exchanged in an MFI-Type Zeolite. *ACS Appl. Mater. Interfaces* **2016,** *8* (13), 8821-8833, DOI: 10.1021/acsami.6b00909.
(7) Belmabkhout, Y.; Serna-Guerrero, R.; Sayari, A. Amine-Bearing Mesoporous Silica for CO_2 Removal from Dry and Humid Air. *Chem. Eng. Sci.* **2010,** *65* (11), 3695-3698, DOI: 10.1016/j.ces.2010.02.044.
(8) Kumar, A.; Hua, C.; Madden, D. G.; O'Nolan, D.; Chen, K. J.; Keane, L. J.; Perry, J. J.; Zaworotko, M. J. Hybrid Ultramicroporous Materials (HUMs) with Enhanced Stability and Trace Carbon Capture Performance. *Chem. Commun.* **2017,** *53* (44), 5946-5949, DOI: 10.1039/c7cc02289a.
(9) Bhatt, P. M.; Belmabkhout, Y.; Cadiau, A.; Adil, K.; Shekhah, O.; Shkurenko, A.; Barbour, L. J.; Eddaoudi, M. A Fine-Tuned Fluorinated MOF Addresses the Needs for Trace CO2 Removal and Air Capture Using Physisorption. *J. Am. Chem. Soc.* **2016,** *138* (29), 9301-9307, DOI: 10.1021/jacs.6b05345.